مدينة زويل للعلوم والتكنولوجيا
Zewail City of Science and Technology

School of Engineering

SPC 317 Fluid Mechanics II

Project Report:
CFD Analysis of NACA0015 Airfoil

Name	Student ID	Email
Abdelrahman Mohamed	202200281	s-abdelrahman.alnaqeb@zewailcity.edu.eg
Marwan Amr	202200050	s-marwan.abdelmegid@zewailcity.edu.eg

Submitted to:
Dr. Ahmed Alatyar

January 2025

Abstract

The text discusses the design and analysis of airfoils, specifically those developed by NACA. Airfoils are critical in determining aerodynamic forces, which are influenced by their shape and orientation. Designers often optimize these shapes using simulations or select from existing data. NACA airfoils, developed during 1929-1947, combine thickness envelopes with camber lines and remain essential for aerodynamic research.

The document focuses on the NACA0015 airfoil, a symmetric airfoil with no camber. It outlines the process of constructing this airfoil using specific equations and simulates its aerodynamics using computer programs. The simulation involves defining conditions, plotting the airfoil using tools like Ansys, defining grid meshes (chosen to be a C-grid), and using the SST model for analysis.

Results from the simulation are compared to experimental data on the NACA0015 at various angles of attack, considering variables like Reynold's number. It was noted that errors in simulations might stem from differences in geometric dimensions or mesh used. The report highlights the importance of matching experimental conditions to improve accuracy in simulations.

Contents

Chapter 1

Introduction

1.1 The airfoil

defined as a slice of a wing:

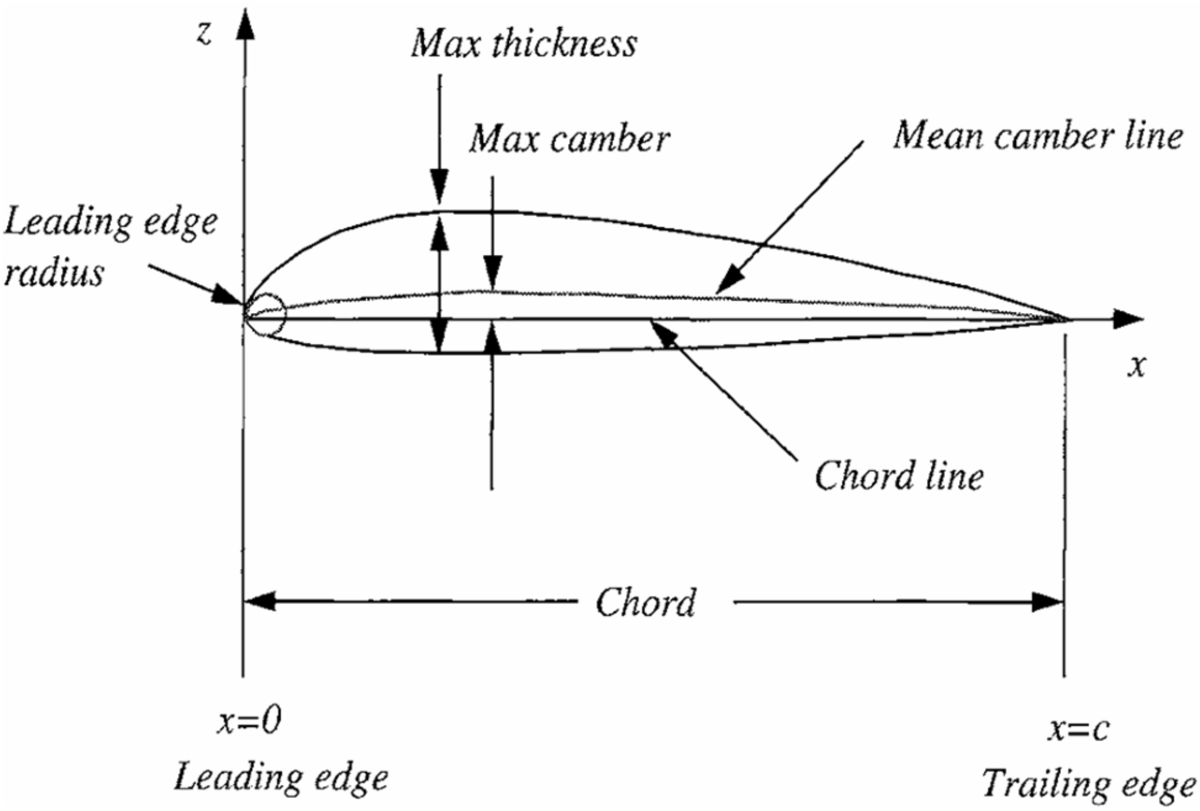

Figure 1.1: Nomenclature of an airfoil [1]

determines the aerodynamic forces on an airfoil, along with its boundary-layer profiles, transition, and separation characteristics, are determined by its shape and orientation. Aircraft designers invest significant effort in optimizing airfoil shapes for specific designs, often using computer programs. Alternatively, airfoil shapes may be selected from published geometry and performance data. These shapes are frequently categorized into families with gradual variations in shape-defining parameters.

Figure 1.1 illustrates a typical airfoil and its descriptive parameters. The chord line, a straight line from the leading to the trailing edge, defines the airfoil's chord length (c). The mean camber line is a curved line equidistant between the upper and lower surfaces, with the maximum camber being the greatest distance between the chord and mean camber lines. A symmetrical airfoil has a mean camber line coinciding with its chord line. The airfoil's shape is further characterized by a thickness envelope around the mean camber line, defined by parameters such as maximum thickness (as a fraction of chord length), its location, and the leading-edge radius.

1.2 Lift and Drag coefficients

Lift and drag generated by any airfoil are usually measured in a wind tunnel, or simulated (as is this report's case) and released publicly as coefficients, where lift and drag coefficients are defined as follows:

$$C_L = \frac{L}{\frac{1}{2}\rho v^2 A} \tag{1.1}$$

and

$$C_d = \frac{F_d}{\frac{1}{2}\rho v^2 A} \tag{1.2}$$

Where

L is the lift force, which is the force acting perpendicular to the oncoming flow direction.

F_d is the drag force, which is the force acting parallel to the oncoming flow direction.

ρ is the air density.

v is the velocity of the airflow relative to the airfoil.

A is the reference area, typically the wing area or airfoil planform area for which the lift and drag are being calculated.

Since an airfoil, defined as a slice of a wing, has no planform area, wind tunnel tests use a wing section, often spanning the entire test section, as shown in Fig. 1.1.

1.3 The NACA0015 airfoil

The NACA airfoils, developed from 1929 to 1947 under Eastman Jacobs at NACA's Langley Field Facility, were based on simple geometric descriptions of section shapes. Despite advancements in airfoil design using modern computational methods, NACA airfoils remain valuable for aerodynamic studies.

NACA airfoils combine a thickness envelope with a camber line. The equations describing this process are: [2]

$$X_u = X - Y_t(X)\sin\theta \tag{1.3}$$

$$Y_u = Y_c(X) + Y_t(X)\cos\theta \tag{1.4}$$

and

$$X_L = X + Y_t(X)\sin\theta \tag{1.5}$$

$$Y_L = Y_c(X) - Y_t(X)\cos\theta \tag{1.6}$$

Here, $Y_t(X)$ is the thickness function, $Y_c(X)$ is the camber line function, and:

$$\theta = \tan^{-1}\left(\frac{dY_c}{dX}\right) \tag{1.7}$$

The camber line slope (θ) is often neglected to simplify calculations, making it easier to derive the thickness envelope and camber line for a given airfoil.

To construct our NACA0015 airfoil, we have our thickness function[3]:

$$Y_t(X) = \frac{t}{0.2}\left[0.2969\sqrt{X} - 0.1260X - 0.3516X^2 + 0.2843X^3 - 0.1015X^4\right]$$

Here $t = 0.15$, and X, the chord position, is going to range from 0 to 1. The NACA0015 airfoil doesn't have any camber since it's symmetric, therefore, we substitute $Y_c(X) = 0$ and $\theta = 0$ in our equations describing the NACA airfoils. Doing so we get:

$$X_u = X$$

$$Y_u = Y_t(X)$$

$$X_L = X$$

$$Y_L = -Y_t(X) \quad \text{(symmetric airfoil)}$$

Implementing the above in a python function gives:

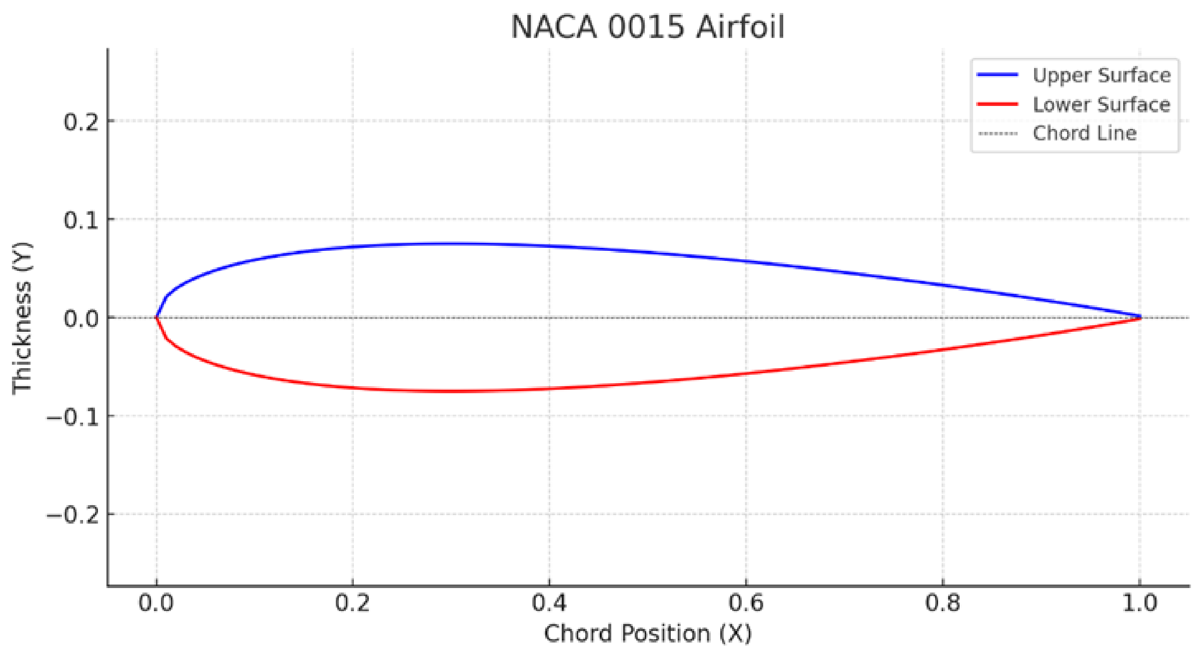

Figure 1.2: NACA0015 airfoil implemented in the cartesian plane using the above functions

Chapter 2

The simulation

2.1 Introduction

As explained above, we use the data to simulate our airfoil with the given conditions. We first need to give our conditions for the simulation, which we do so below:

Velocity	adjusted based on Reynold's numbers
Density of air	$1.225\ \frac{kg}{m^3}$
Viscosity of air	$0.000017894\ \frac{kg}{m \cdot s}$
Chord length	1 m
y^+	≤ 1
Reynold's Number	$0.36 \cdot 10^6, 0.5 \cdot 10^6, 0.68 \cdot 10^6$

We also plot the airfoil for use in Ansys:

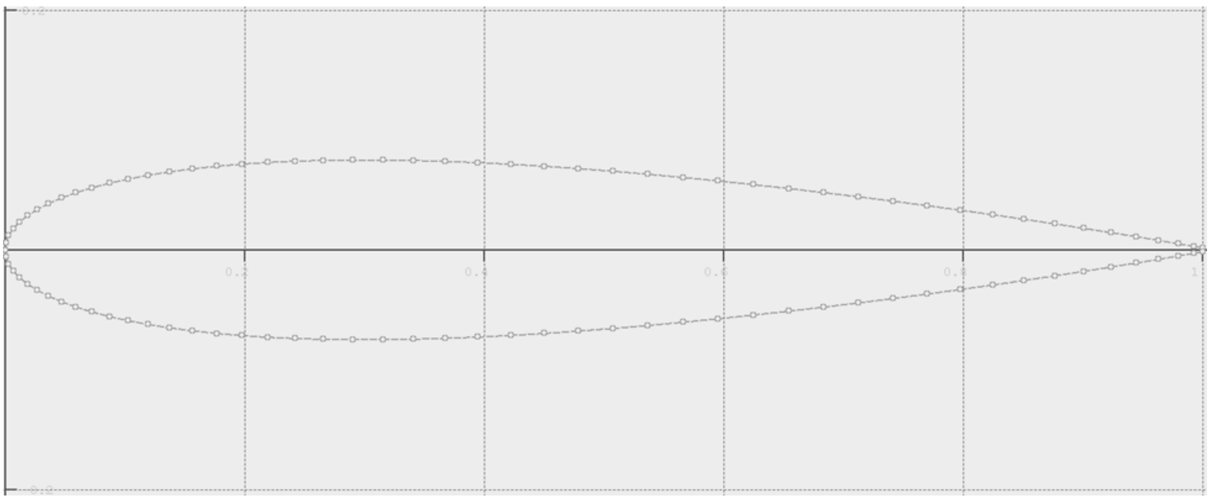

Figure 2.1: NACA0015 airfoil plotted using 100 points on xFoil5

2.2 Pre-processing

This is the phase where the geometry, boundary conditions, mesh, control surface, etc... is defined.
We already defined the geometry in the introduction and the previous section. Therefore, we go directly to the analysis.

2.2.1 Meshing

There are many types of meshes we can use for the simulation. One example is the O-grid mesh:

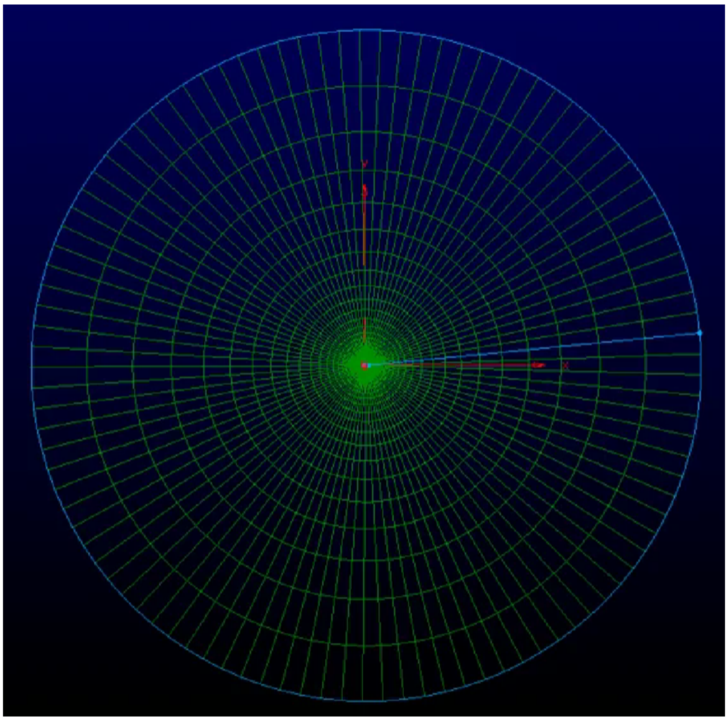

Figure 2.2: O-grid mesh on NACA0015 airfoil (made using Cadence Fidelity Pointwise

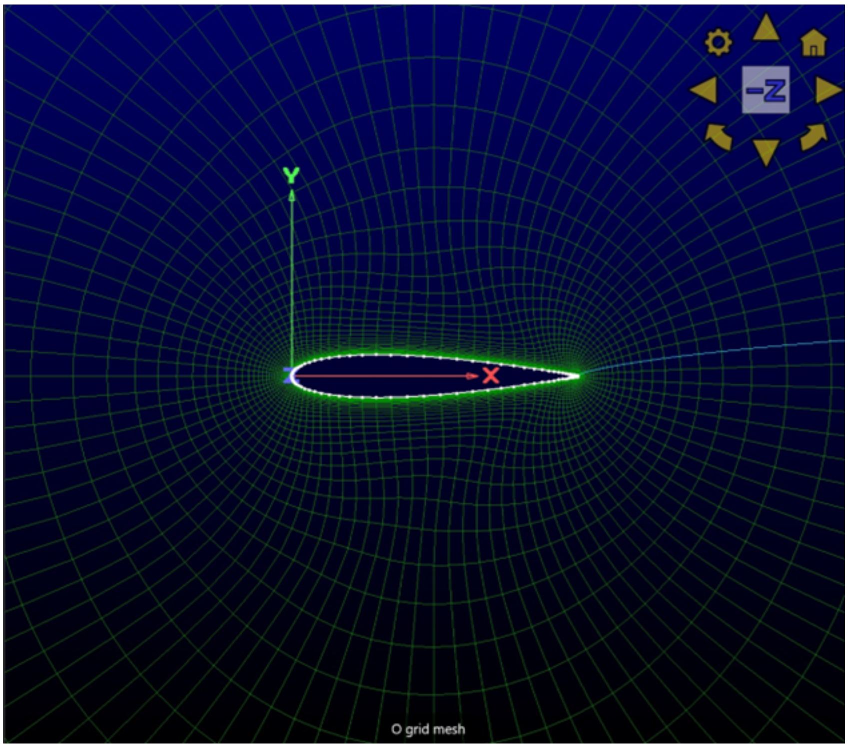

Figure 2.3: Zoomed in for better quality

However, we end up choosing a C-grid mesh because it can capture separation and wake more effectively.

That said, here is our C-grid mesh:

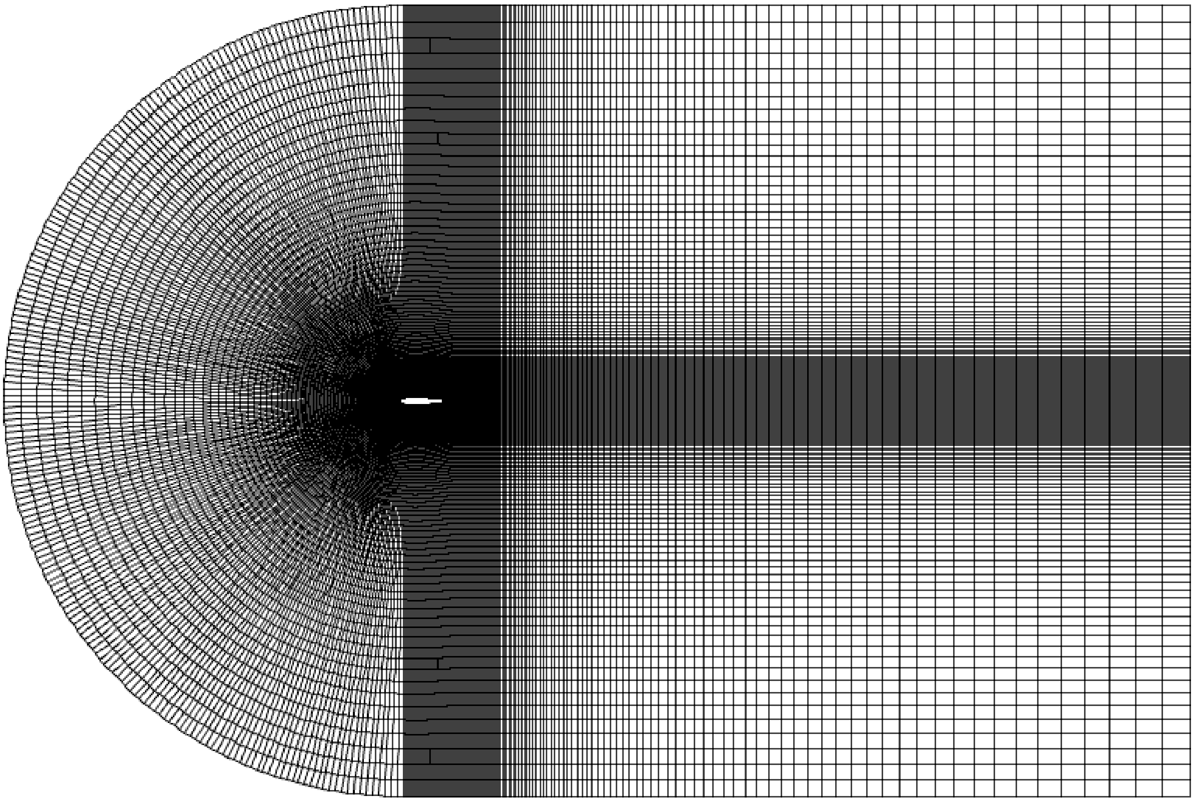

Figure 2.4: C-grid mesh (made using Ansys)

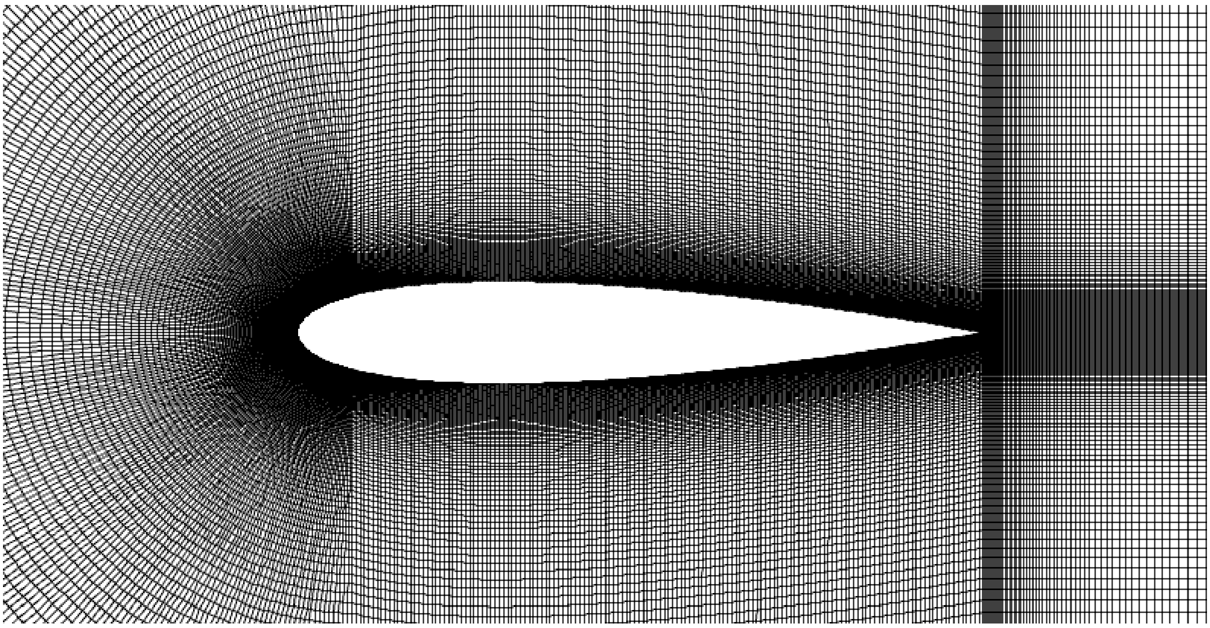

Figure 2.5: Zoomed in C-grid mesh

2.2.2 Selecting a solver

We use the $k - \omega$ SST model, both in steady and transient modes with the pressure model.

2.2.3 Boundary Conditions

already specified in section 2.1.

2.3 Post-processing

The data is gathered and discussed in the following sections.

Chapter 3

Results and Discussion

3.1 Experimental data on the NACA0015 airfoil at $\alpha = 35^o$

Before discussing our simulation results, we show the experimental data on the NACA0015 airfoil at an AoA of 35^o.

using the findings from [4], we have a C_l and C_d vs α (angle of attack) charts shown below:

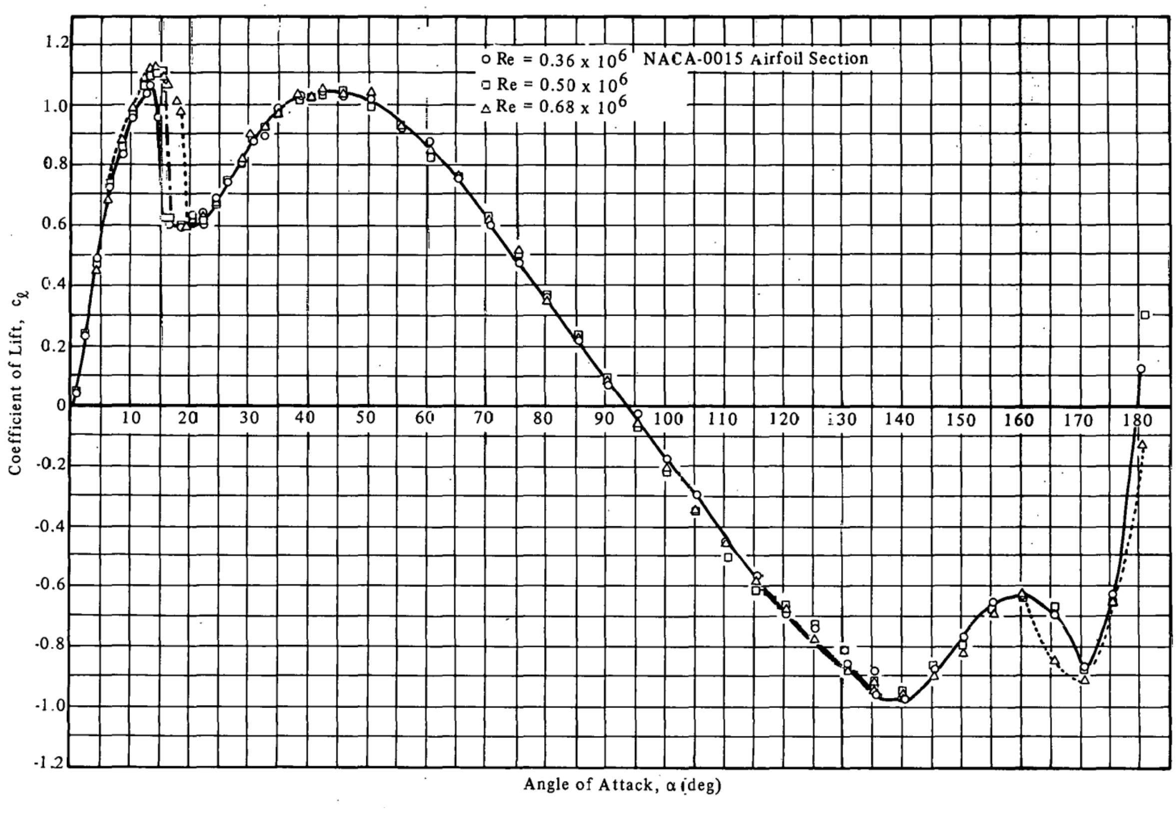

Figure 3.1: Full Range section Lift Coefficients for the NACA-0015 Airfoil at Reynolds Numbers $0.36 \cdot 10^6$, $0.5 \cdot 10^6$, and $0.68 \cdot 10^6$

From this chart, the list coefficients at $\alpha = 35^o$ are as follows:

Re	C_l
$0.36 \cdot 10^6$	0.9800
$0.5 \cdot 10^6$	0.9800
$0.68 \cdot 10^6$	0.9800

similarly, for drag coefficients,

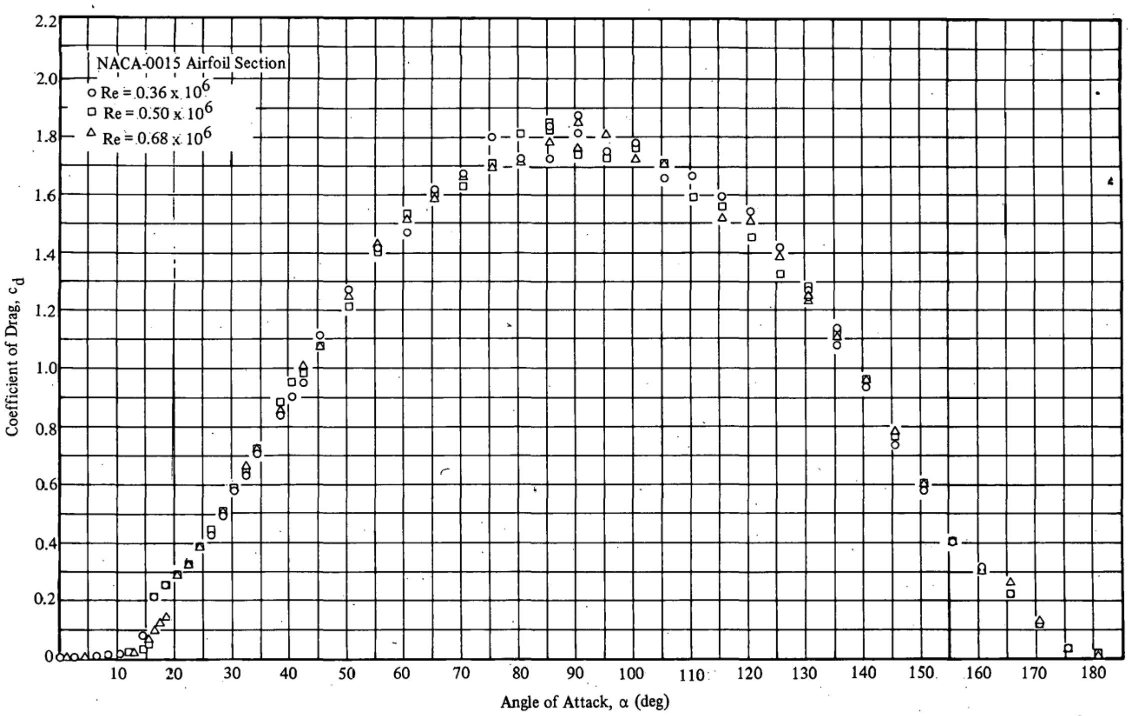

Figure 3.2: Full Range section Drag Coefficients for the NACA-0015 Airfoil at Reynolds Numbers $0.36 \cdot 10^6$, $0.5 \cdot 10^6$, and $0.68 \cdot 10^6$

Re	C_d
$0.36 \cdot 10^6$	0.7450
$0.5 \cdot 10^6$	0.7450
$0.68 \cdot 10^6$	0.7450

From that we find that experimentally, the lift coefficient is approximately independent of Reynold's number at $\alpha = 35^o$.

We also note that the airfoils in the experiment had "6 in. (15.24-cm) chords with a 3-ft (0.91-m) span". [4]
Which makes their planform area at $\alpha = 0^o$ be $15.24 \cdot 10^{-}2 \cos 35^0 \times 0.91 = 0.1136m^2$, Since we have chosen a chord length of 1m, we make our span 5.971m to have the same aspect ratio as in the experients, whose area is $4.891m^2$ which we use for calculating the coefficients for our simulations.

multiplying the result by

3.2 Simulation results

3.2.1 Steady flow

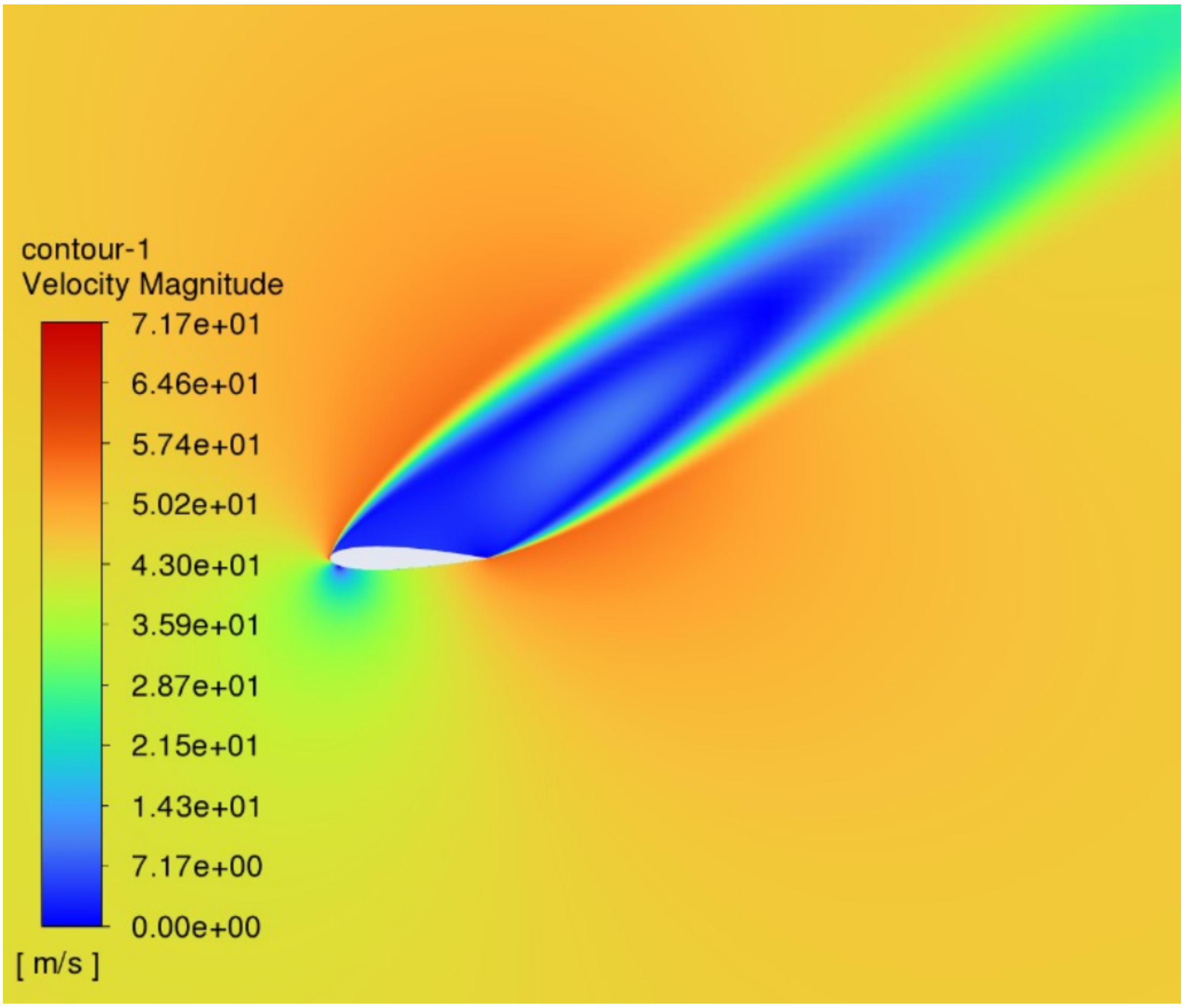

Figure 3.3: Velocity contour of our first simulation (steady)

which gives us a C_d of 0.5411 and a C_l of 0.7292.
Errors could be from the mesh and the steady model used for the simulation.

3.2.2 Unsteady flow

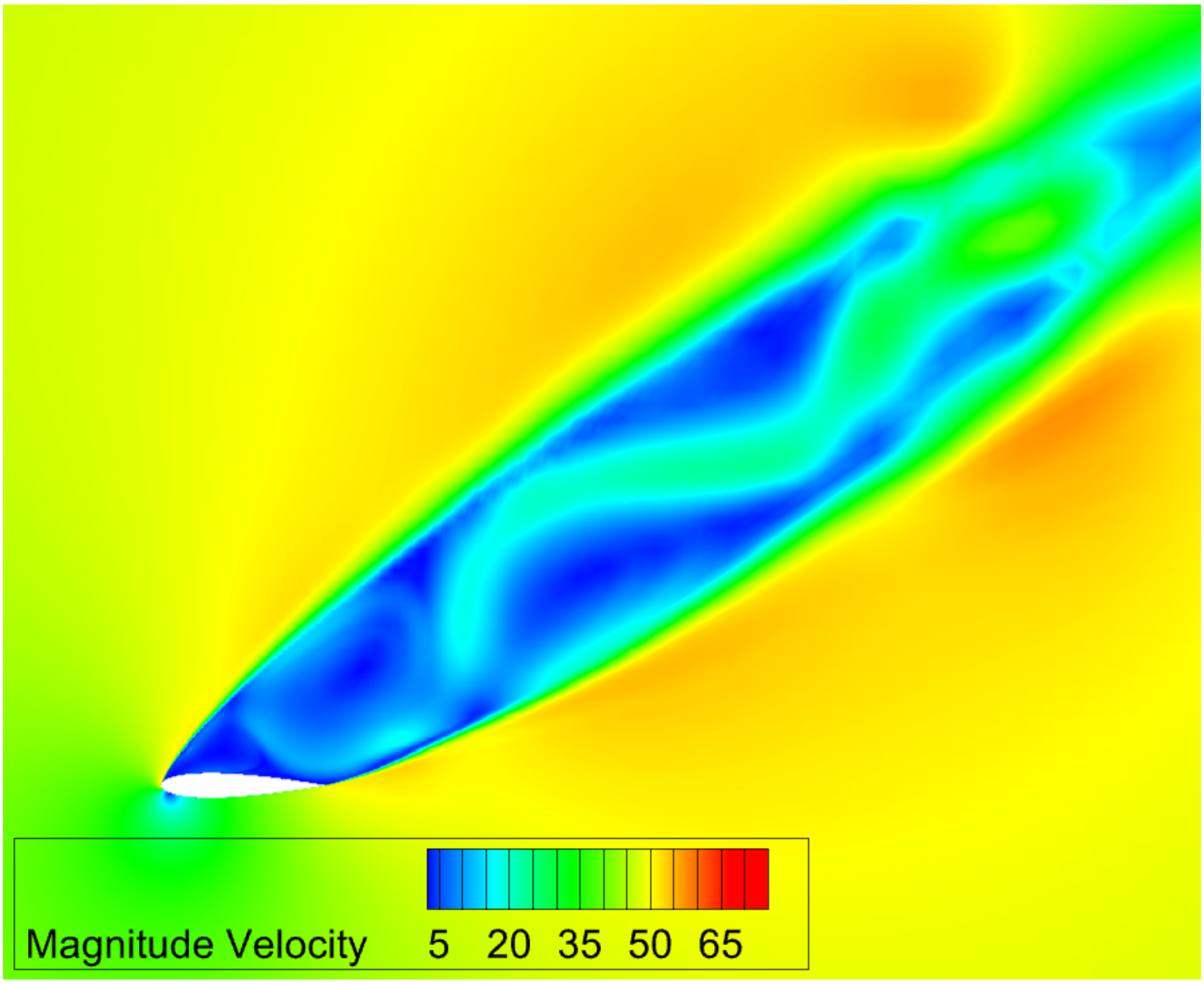

Figure 3.4: Velocity contour for unsteady flow

Doing the simulation for all reynold's numbers, then doing the calculation to find the lift and drag coefficients yields us:

Re	Lift (N)	Drag (N)	C_l	C_d
0.36×10^6	239.60128	177.99724	0.20358937	0.15176203
0.5×10^6	462.61811	346.32414	0.39308324	0.29527407
0.68×10^6	857.41122	633.12866	0.72854823	0.5398183

Table 3.1: Lift and Drag Coefficients for NACA0015 Airfoil at Different Reynolds Numbers

Although we maintained the aspect ratio of our airfoil with the experiment's errors still exist.
We recommend using a momentum-based model instead of a distance based Rhie-Chow model. Since most of the lift and drag are momentum based instead of distance/friction based.

Bibliography

[1] Brandt, Steven A., et al., *Introduction to Aeronautics: A Design Perspective, Second Edition*, 2004.

[2] Abbott, I.H., and von Doenhoff, A.E., *Theory of Wing Sections*, Dover, 1959.

[3] Jacobs, Eastman Nixon, Kenneth Edwards Ward, and Robert McLean Pinkerton, *The Characteristics of 78 Related Airfoil Sections from Tests in the Variable-Density Wind Tunnel*, No. 460, US Government Printing Office, 1933.

[4] Sheldahl, R.E., and Klimas, P.C., *Aerodynamic Characteristics of Seven Symmetrical Airfoil Sections Through 180-Degree Angle of Attack for Use in Aerodynamic Analysis of Vertical Axis Wind Turbines*, [Online]. Available: https://www.osti.gov/servlets/purl/6548367/, accessed Dec. 31, 2024.

The End